Indian J. Phys. **81 (10)** 1079-1093 (2007)

IJP

Electronic structure of ZnS nanotube : a density-functional study

Sougata Pal, Biplab Goswami and Pranab Sarkar*

Department of Chemistry, Visva-Bharati University, Santiniketan-731 235, West Bengal, India

E-mail pranab_69@yahoo co in

Abstract : We present results of our theoretical calculations on structural, electronic and optical properties of ZnS nanotube The calculations are performed by using density-functional tight-binding (DFTB) method. We have considered both single-walled and double-walled nanotubes and studied the variation of radial distribution, Mulliken population, density of states and band gap as functions of both tube radius and tube helicity.

Keywords : ZnS nanotube, single and double walled, electronic structure

PACS Nos. : 72.80 Rj, 73.20.At, 61.46.+w

1. Introduction

One-dimensional (1D) nanostructures such as semiconductor nanowires or nanotubes are of fundamental importance because of their potential use in both nanoscale engineering and nanotechnology [1–3]. Properties of these 1D nanostructures may sensitively depend on their structures, morphologies and sizes. The discovery of carbon nanotubes in 1991 [4] has stimulated extensive experimental and theoretical research concerning structures based on hexagon networks. The physical properties of carbon nanotube depends on the diameter as well as the helicity of the nanotube. Thus the armchair (n,n) carbon nanotubes are metallic while zigzag (n,0) carbon nanotubes are semiconducting [5–8]. The band gap can also be controlled by varying the diameter of the tube, thus allowing band gap engineering. The last couple of decades have witnessed an exponential growth of activities in this field, driven both by excitement of understanding new science and by the potential hope for technological applications. Recently, nanotubes made by non-carbon based inorganic semiconductor nanostructures popularly known as inorganic nanotubes have become the subject of extensive studies [9]. Their potential applications range from highly high porous catalytic and ultralight

*Corresponding Author

anti-corrosive materials to electron field emitters and non-toxic strengthening fibers. The helical structure of nanotubes, with their semiconducting behavior and optical activity, opens up possible applications in nonlinear optics and solar-cell technology. The first successful report [10] on inorganic (WS_2) nanotubes was made by Tenne in 1992 followed by intense experimental and theoretical research on hollow cylindrical structures that led to the development of numerous inorganic nanotubes [11–20] with diverse properties. In 1994, Rubio *et al* [11] predicted the possibility of existence of tubulenes based on hexagonal boron nitride (BN). Their dielectric properties were presumed to remain stable upon changes in their geometrical characteristics. This prediction was very important for the development of nanoelectronics, it initiated numerous studies on the synthesis of such nanotubes. The same group had also studied the electronic structure of GaSe nanotubes [12]. It has also been revealed that tubular structures of III-V compounds such as AlN [13], GaN [14], GaAS [15] display the electronic properties which are quite different from their bulk materials. Zhao *et al* [16] theoretically studied strain energy, geometries and electronic structure of SiC nanotubes. They have showed that SiC nanotubes are semiconducting, the band gap of which increases with increasing tube diameter.

Zinc sulfide (ZnS) is an important II-IV semiconductor with a wide band gap energy of 3.66 eV. ZnS nanocrystals have attracted tremendous attention because of their application in diverse fields. Thus they can be used as a key material for ultraviolet light-emitting diodes and injection lasers, as phosphors in cathode-ray tube and flat panel displays, for thin film electro-luminescence, and for IR windows [21–23]. ZnS nanocrystals have also been investigated for use in fuel cells, solar energy conversion, catalysts and non-linear optical devices. Much effort has gone into the synthesis and characterization of 1D nanocrystals and nanoparticles of ZnS. Wang *et al* [24] have used ZnO nanobelts as templates to fabricate ZnS nanotubes by chemical reaction between ZnO supports and H_2S. Recently, Zhu *et al* [25] have also reported the synthesis of ZnS nanotube. Jiang *et al* [26] reported the ZnS nanowire with a wurtzite poly-type modulated structure. Zhang *et al* [27] described a synthetic method for the preparation of ZnS nanotube assisted by carbon nanotubes. They have shown that the UV-vis absorption spectra of these nanotubes exhibit large blue shifts because of quantum size effects. These 1D nanostructures of ZnS may have potential applications in high H_2 storage, drug delivery and second order template because of their large capacity and high solubility. Although, there are number of experimental studies on the synthesis and characterization of ZnS nanotubes, theoretical research addressing the electronic structure of ZnS nanotubes and their dependence on the chirality and diameter are scarce. In a recent paper [28] we have studied the structural and energetic properties *viz.* strain energy, buckling, band gap *etc.* of single-walled ZnS nanotube. In the present communication we propose to study the electronic structure of single-walled ZnS nanotube (SWZnSNT) in more detail and also of double-walled ZnS

nanotube (DWZnSNT). Double-walled nanotubes exhibit different structural characteristics from single-walled nanotubes (SWNT) and the interwall interaction could play an important role in the structural, electronic and optical properties of double-walled nanotubes (DWNT). We will address, radial distribution, Mulliken population, density of states (DOSs) and band gap for both single-walled and double-walled nanotube as a function of the tube radius and also as helicity of the tube. Admittedly, the present study is a natural and relevant extension of our earlier work [28].

2. Theoretical method

We employed the parametrized density-functional tight-binding method due to Porezag *et al* [29] which has been described in details elsewhere, and, therefore, here shall be only briefly outlined. In this method the hopping integrals used to construct the Hamiltonian and overlap matrices are tabulated as a function of internuclear distance on the basis of first principles density-functional theory with local density approximation. The method employs the localized basis sets, retaining only one and two-center contributions to the Hamiltonian matrix elements. A minimal basis set corresponding to a single atomic like orbital per atomic valence state is used. The total energy is written as the sum of all occupied Kohn-Sham energies which represents the 'band-structure' energy and the repulsive two-center terms between the atoms located at R_j and R_k as follows :

$$E = \sum^{occ} \epsilon_i + \frac{1}{2} \sum_j \sum_{k \neq j} U_{jk} \left(\left| \boldsymbol{R}_j - \boldsymbol{R}_k \right. \right. \tag{1}$$

The pair potentials U_{jk} are determined so that the total energy curves of the diatomics are well reproduced. This approach has been shown to be a good compromise between the more accurate, but more costly, *ab initio* techniques, and computationally less expensive, but less accurate, empirical potentials. Its applicability to the study of the electronic structure of nanotubes has already been shown for several tubular systems [14–18,28]. For each ZnS tubular structure having different radius and helicity, a series of calculations have been carried out in which the initial structure was fully relaxed with respect to both the atomic positions and the tube cell length using conjugate gradient technique. The periodic boundary conditions along the tube axis was employed with a vacuum region ($\approx$ 8.0 Å) between neighbouring tubes to avoid significant interactions between the periodic images. Using the nonorthogonal TB scheme briefly outlined above we have performed a series of calculations aimed at characterizing the properties of ZnS nanotubes. In particular, we have considered zigzag (n,0) and armchair (n,n) nanotubes. The structure of a single-wall nanotube can be conceptualized by wrapping a one-atom-thick layer of graphite called graphene into a seamless cylinder. The way the graphite sheet is wrapped is represented by a pair of indices (n,m) called chiral vector. The integers n and m denote the number of unit vectors along two directions

in the honeycomb crystal lattice of graphene. If $m = 0$, the nanotubes are called zigzag and if $n = m$, the nanotubes are called armchair.

3. Results and discussion

Single-walled nanotube :

In Figure 1 we have shown the optimized structure of two representative (a) armchair (8,8) and (b) zigzag (14,0) single-walled ZnS nanotubes. The average Zn-S bond lengths in zigzag and armchair nanotubes are 2.33 Å and 2.30 Å respectively. These bond lengths are slightly shorter compared to 2.34 Å in the bulk which is primarily a

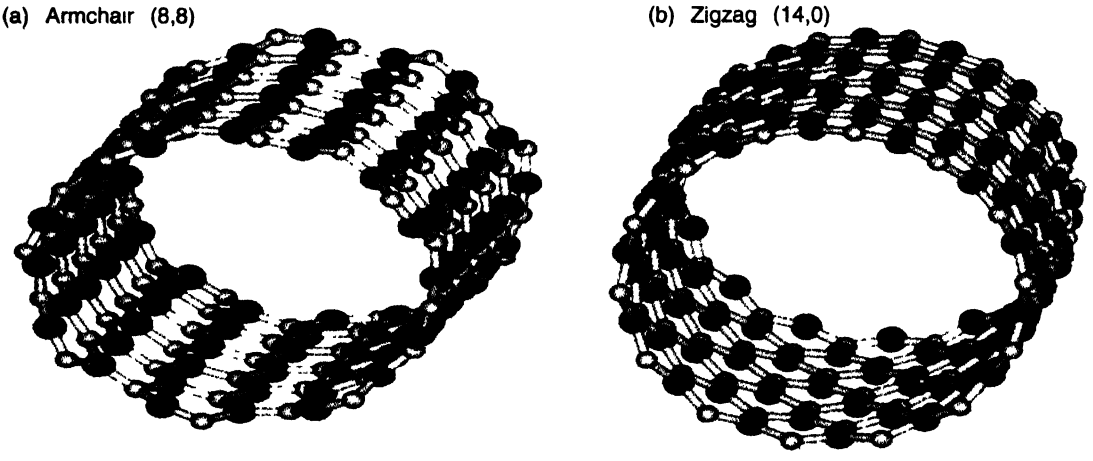

Figure 1. Optimized geometry of SWZnSNTs : (a) (8,8) armchair nanotube and (b) (14,0) zigzag nanotube

consequence of the lower coordination numbers in the tube compared to bulk. In describing the structural properties of the nanotubes we first define a line passing through the center of the ZnS nanotube through

$$\boldsymbol{R}_0 = \frac{1}{n+m}\sum_{j=1}^{n+m}\boldsymbol{R}_j, \tag{2}$$

where '*n*' and '*m*' are number of Zn and S atoms in the nanotube. Subsequently, the radial distance for the *j*-th atom is defined as

$$r_j = \left|\boldsymbol{R}_j - \boldsymbol{R}_0\right|, \quad j = 1,\ 2, \ldots n+m\,. \tag{3}$$

Figure 2 shows the radial distributions of Zn and S atoms in ZnS nanotubes of varying sizes with either zigzag (left panel) and armchair (right panel) symmetry. The Zn and S atoms which are at same distance from the center of the tube in the initial geometry has splitted into two groups in the optimized geometry. The inspection of individual radial distribution shows that Zn atoms are lying relatively inner side from the surface whereas the S atoms are at relatively outer side. This feature is exactly the same as that had been observed in ZnS quantum dots [30]. This causes the presence

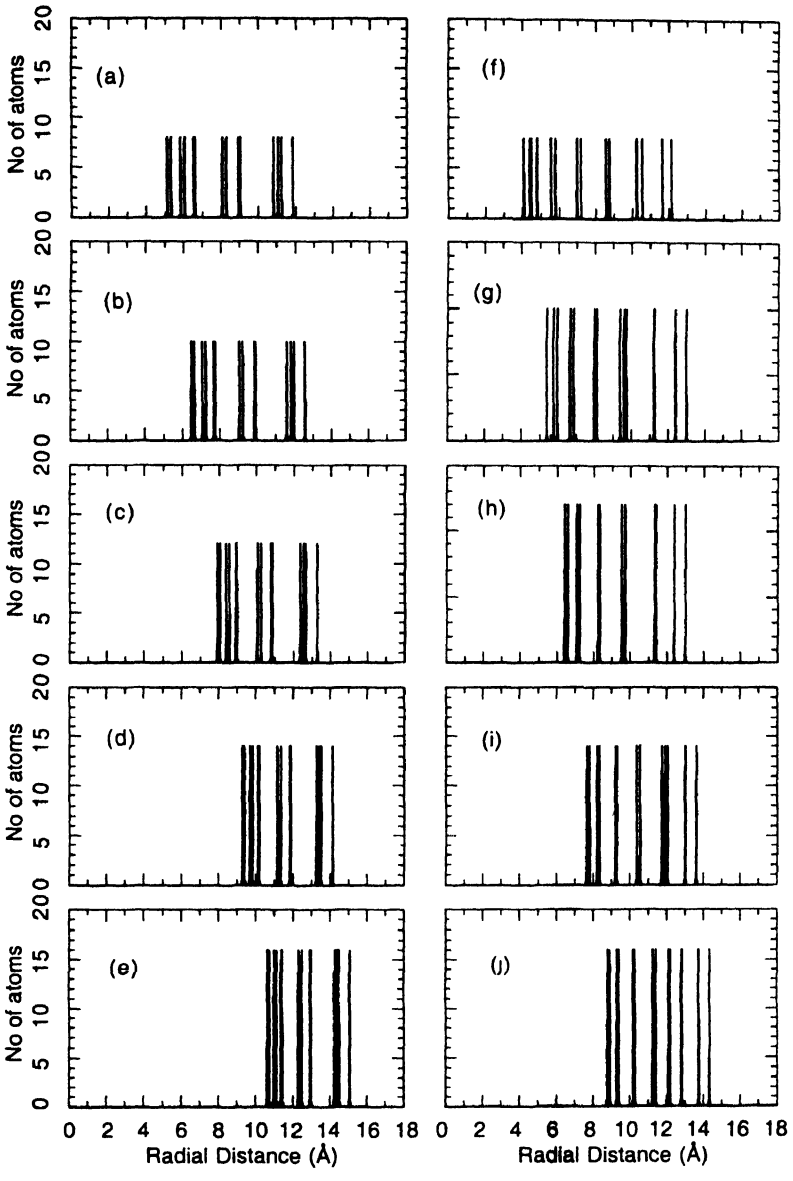

Figure 2. Radial distribution of Zn and S atoms for zigzag (left panel) and armchair (right panel) SWZnSNTs of different size : (a) (8,0), (b) (10,0), (c) (12,0), (d) (14,0), (e) (16,0), zigzag nanotubes and (f) (4,4), (g) (5,5), (h) (6,6), (i) (7,7), (j) (8,8) armchair nanotubes.

of certain degree of buckling on the tube surface and this tendency of buckling of ZnS nanotubes is the result of the slightly different hybridizations of Zn and S atom in the curved hexagonal layer. Hernandez *et al* [19] have also found the same kind of buckling effect in BN nanotubes. A close look at the radial distribution reveals that as the radius of the tube increases the separation between Zn and S atoms goes on decreasing both for zigzag and armchair nanotubes. So the extent of buckling decreases with the size

of the tube and its magnitude is slightly dependent on the helicity of the tube. The presence of buckling of these nanotubes may have the effect of forming a surface dipole and hence be highly relevant for potential applications of these nanotubes.

In Figure 3 we have shown the Mulliken gross population of Zn and S atoms for both zigzag (left panel) and armchair (right) nanotubes as a function of radial distance As we have considered only valence electrons in our calculation these numbers would be 12 for Zn and 6 for S. From the figure it is seen that there is almost uniform (other

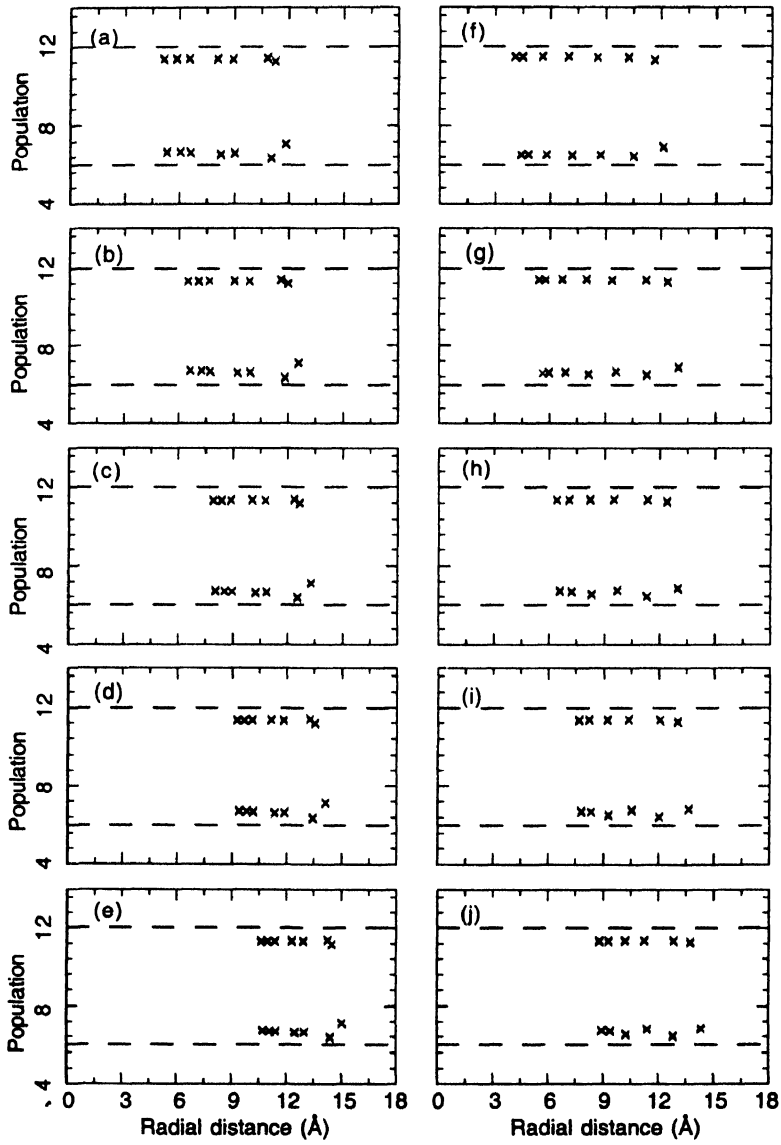

Figure 3. Mulliken population of Zn and S atoms for zigzag (left panel) and armchair (right panel) SWZnSNTs of different size : (a) (8,0), (b) (10,0), (c) (12,0), (d) (14,0), (e) (16,0), zigzag nanotubes and (f) (4,4), (g) (5,5), (h) (6,6), (i) (7,7), (j) (8,8) armchair nanotubes.

than the atoms at both end of the tube) charge transfer from Zn to S and the average charge transfer is about 0.60|*e*| for zigzag and 0.56|*e*| armchair nanotubes. So the study of Mulliken population predicts the ionic nature of the ZnS nanotube similar to other nanotubes like GaN [14], SiC [16], *etc.* and it is independent of the helicity of the tube.

In Figure 4 we have shown the density of states (DOS), obtained by broadening

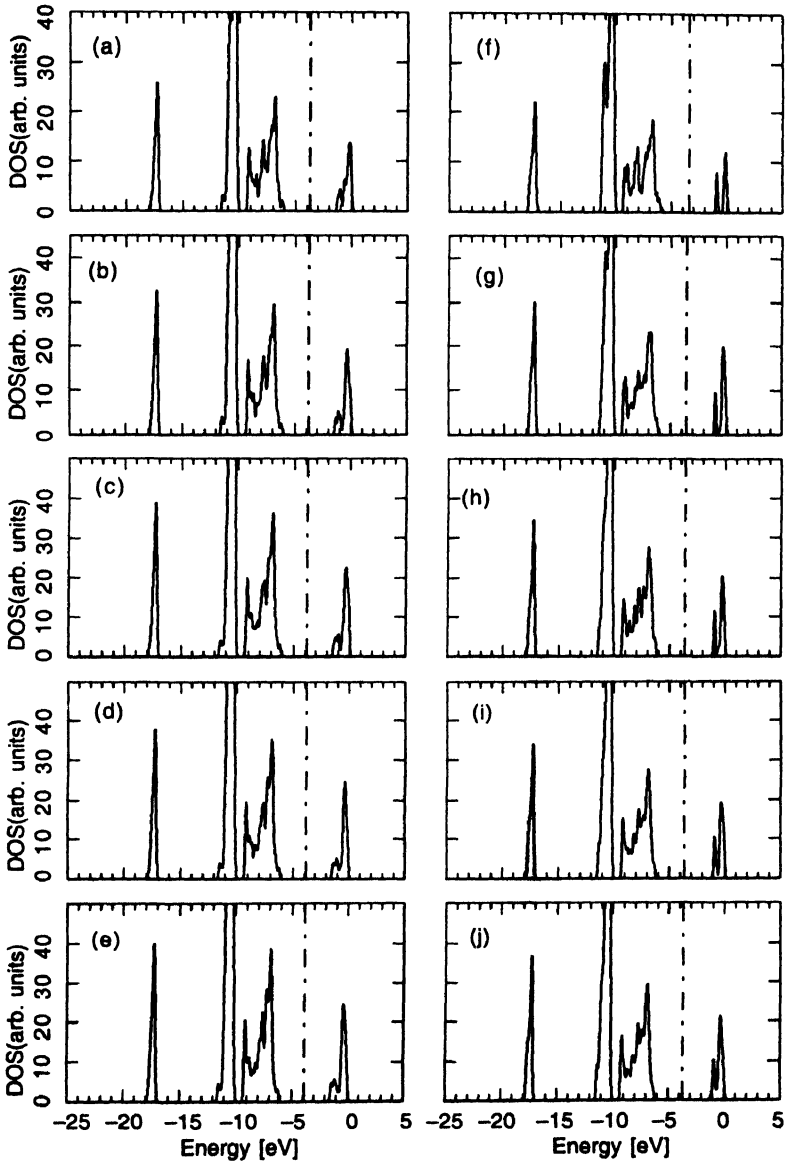

Figure 4. The density of states (DOS) calculated for zigzag (left panel) and armchair (right panel) SWZnSNTs of different sizes : (a) (8,0), (b) (10,0), (c) (12,0), (d) (14,0), (e) (16,0), zigzag nanotubes and (f) (4,4), (g) (5,5), (h) (6,6) (i) (7,7), (j) (8,8) armchair nanotubes.

the individual electronic states slightly with Gaussian for some representative nanotubes of both zigzag (left panel) and armchair (right panel) symmetry. The figure shows that the general feature of the calculated DOS is only weakly influenced by the helicity of the tube. The DOS structure of the lower part (–18 eV to –17 eV) of each valence band is characterized by a large contribution from S 3s states while the higher energy part (–12 eV to –6 eV) of the valence band DOS is dominated by Zn 4s and S 3p states. The conduction band is mainly characterized by Zn 4p contributions. One of the striking differences between the DOSs of these nanotubes to that of ZnS quantum dots (QDs) [30] is that there are no states in the band gap region and hence have higher band gap values than that of QDs.

The evolution of the band gap of zigzag and armchair nanotubes as a function of the radius of the tube is plotted in Figure 5. The magnitudes of the band gap are

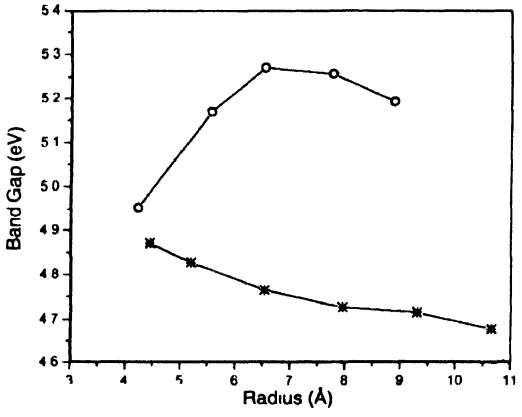

Figure 5. Band gaps of single-walled armchair and zigzag naotubes as a function of the tube radius Circles (0) for armchair and corsses (x) for zigzag naotubes

in good agreement with the experimental values [27] of Zhang *et al.* The armchair nanotubes have higher bandgap values than the corresponding zigzag nanotubes. The nanotubes of AlN [13], GaN [14], SiC [16] and BN [19] also show the similar behaviour. One of the interesting characteristics of ZnS nanotube is that while for zigzag nanotubes the band gap decreases with increasing tube radius it increases for armchair nanotubes. This difference in behaviour of ZnS nanotube may be interpreted as follows. There are two factors responsible for increase or decrease in band gap with tube radius. One is quantum confinement effects that results decrease of bandgap with increasing tube radius and the other factor may be related to curvature induced $\sigma - \pi$ hybridisation [31,32] in nanotubes with different radius. These results imply that the curvature induced $\sigma - \pi$ hybridization has the most pronounced effect for armchair nanotubes resulting in increasing band gap with increasing radius. And for zigzag nanotube it is the quantum size effects that predominates over curvature induced $\sigma - \pi$ hybridization.

Double-walled nanotube :

The optimized structure of double-walled armchair (8,8) and zigzag (14,0)(14,0) ZnS nanotubes are shown in Figure 6. The average Zn-S bond lengths of inner and outer tubes are 2.32 Å and 2.34 Å respectively. In Figure 7 we have shown the radial distribution of both zigzag (left panel) and armchair (right panel) nanotubes of different sizes. The general feature *i.e.* the outward movement of S atoms and inward (towards the tube axis) movement of Zn atoms are nearly the same as that of SWNTs. A careful analysis of the radial distribution reveal that the resulting buckling increases with increasing tube radius for both zigzag and armchair nanotubes. This is in sharp contrast to that of SWNTs where buckling decreases with increasing tube radius.

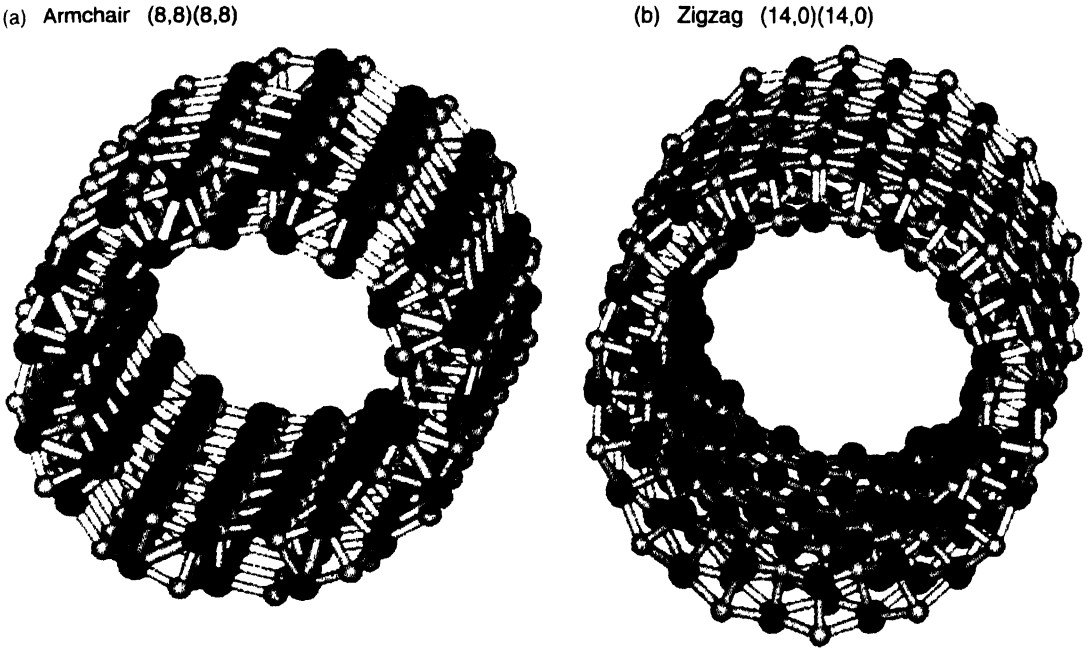

Figure 6. Optimized geometry of DWZnSNTs : (a) (8,8) (8,8) armchair naotube and (b) (14,0) (14,0) zigzag nanotube.

Figure 8 shows the radial distribution of Mulliken population of Zn and S atoms for DWNT as a function of radial distance. If we compare this figure with that of single walled nanotube (Figure 3), a clear distinction is noticed. We observed almost uniform charge transfer through out the whole region of the single walled nanotube while for double-walled nanotube the charge transfer for inner wall atoms are different from that of outer wall. The figure clearly demonstrates that there is relatively more charge transfer from Zn to S in the outer wall than that of inner wall. So the atoms in the outer wall DWNT are more ionic than that of inner wall. A detailed analysis of Mulliken population of individual atoms also show that there is charge transfer from inner wall

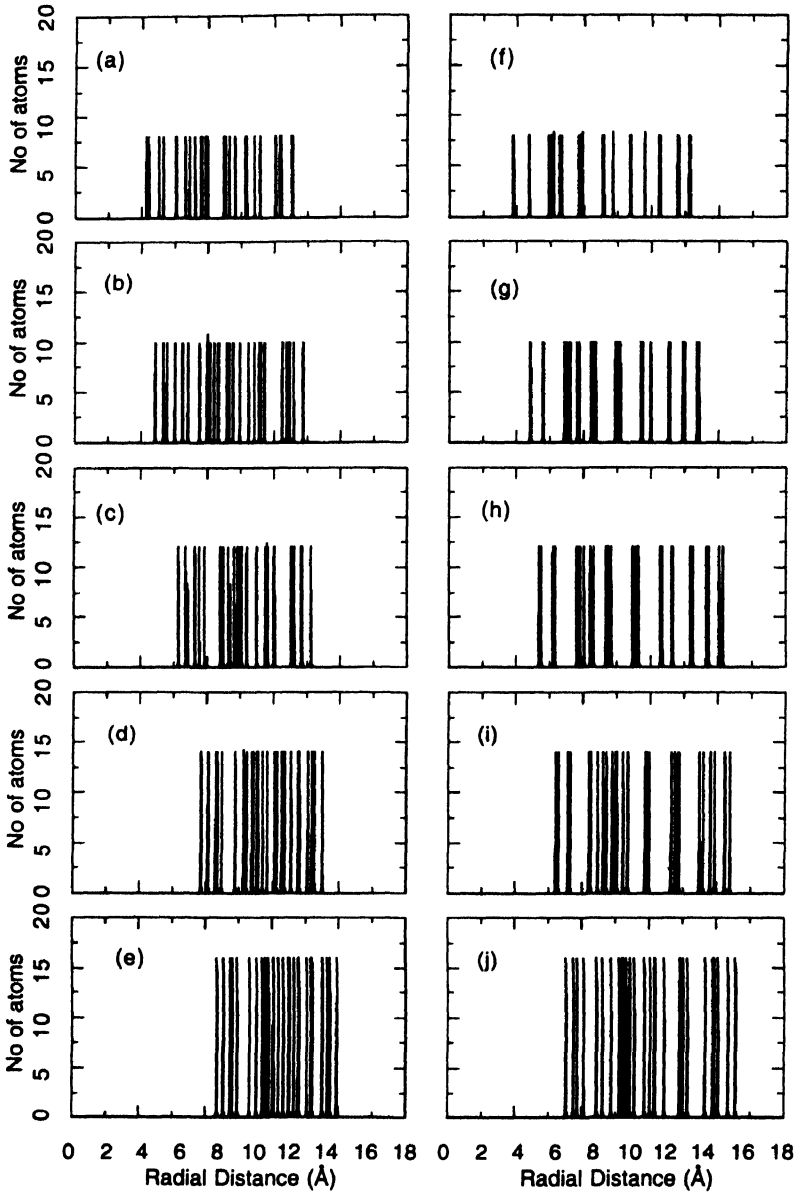

Figure 7. Radial distribution of Zn and S atoms for zigzag (left panel) and armchair (right panel) DWZnSNTs of different size : (a) (8,0)(8,0), (b) (10,0)(10,0), (c) (12,0)(12,0), (d) (14,0)(14,0), (e) (16,0)(16,0), zigzag nanotubes and (f) (4,4)(4,4), (g) (5,5)(5,5), (h) (6,6)(6,6), (i) (7,7)(7,7), (j) (8,8)(8,8) armchair nanotubes.

to outer wall and this is because of the interwall interaction. Liu *et al* [33] also observed similar charge transfer in their study with double-walled boron nitride nanotubes. The magnitudes of charge transfer are higher for zigzag nanotubes compared to armchair nanotubes and also show a clear size-dependent behaviour. It decreases with the increasing radius of the nanotubes.

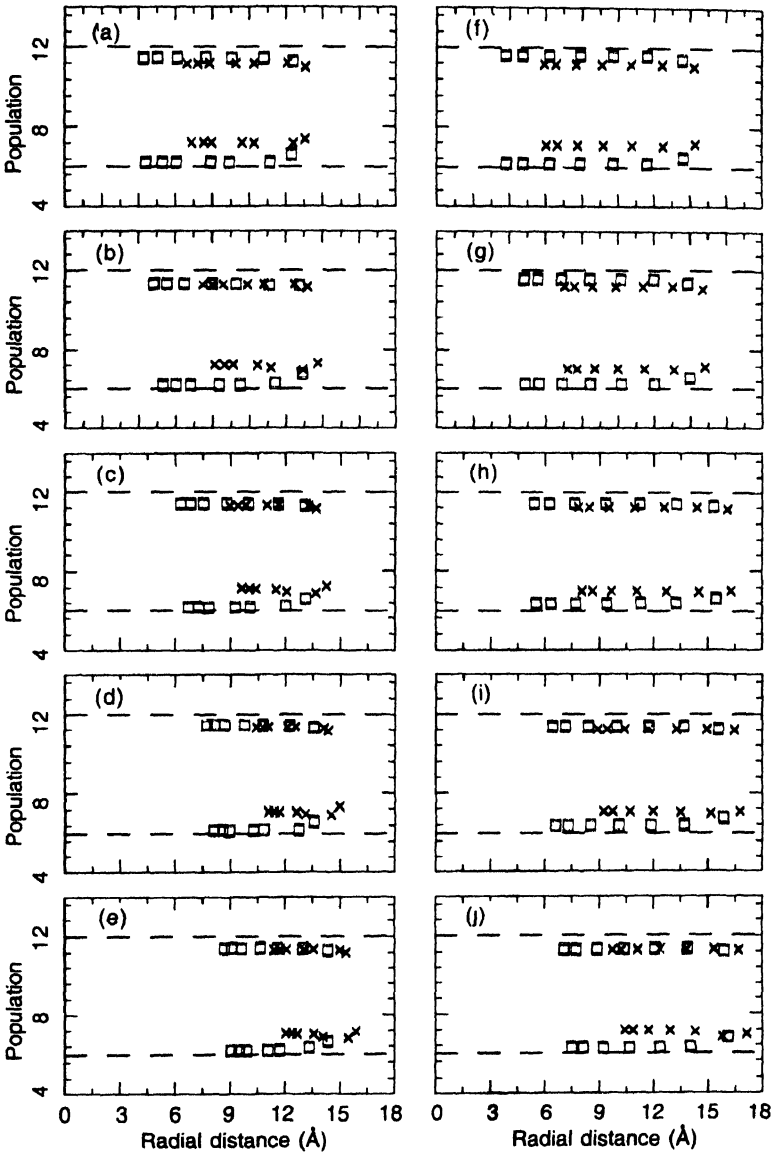

Figure 8. Mulliken population of Zn and S atoms for zigzag (left panel) and armchair (right panel) DWZnSNTs of different size (crosses indicates the population of outer wall atoms and squares, the population of inner wall atoms) : (a) (8,0)(8,0), (b) (10,0)(10,0), (c) (12,0)(12,0), (d) (14,0)(14,0), (e) (16,0)(16,0), zigzag nanotubes and (f) (4,4)(4,4), (g) (5,5)(5,5), (h) (6,6)(6,6), (i) (7,7)(7,7), (j) (8,8)(8,8) armchair nanotubes.

The DOSs of DWZnSNT has shown in Figure 9. The general features are nearly same as that of SWNTs but each band of the DOSs of DWNT are slightly broadened compared to SWNT. The broadening in the DOS clearly indicates the interwall interaction in the nanotubes. If there had not been any interaction, the DOSs of DWNT would be just the sum of DOSs of two SWNTs. A close inspection of the contribution

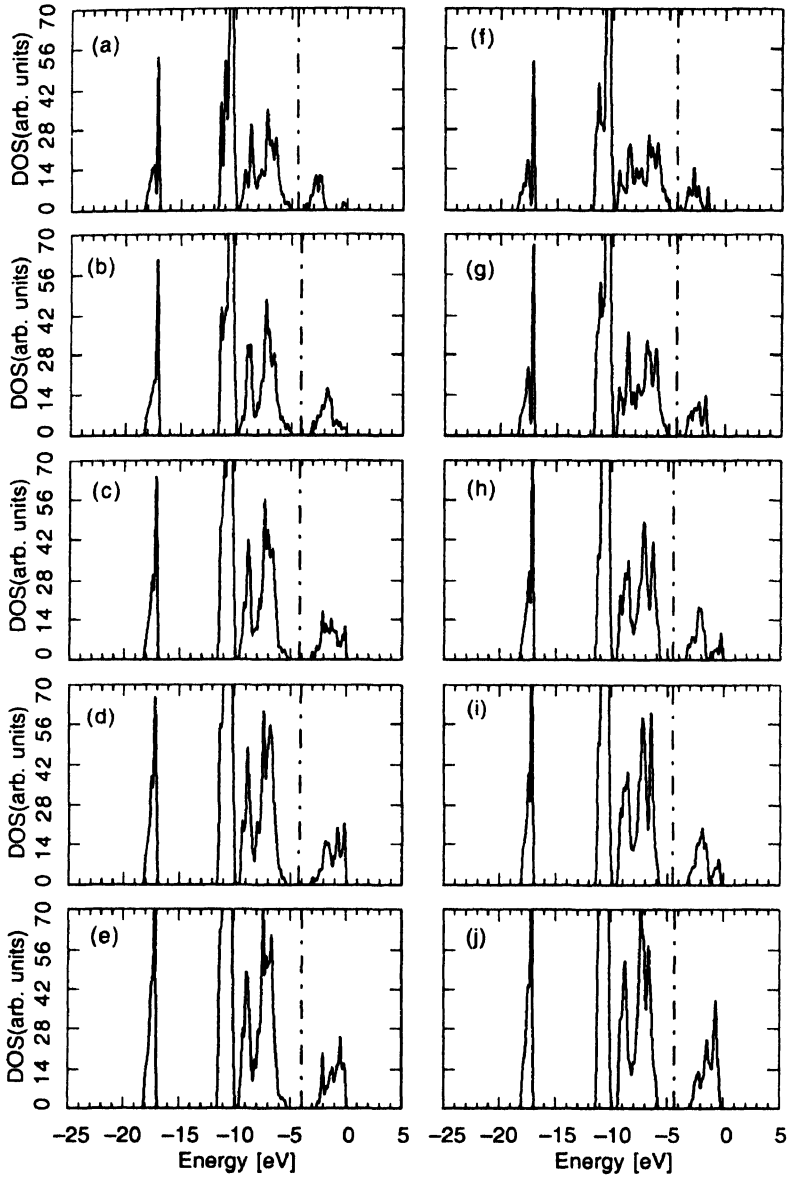

Figure 9. The density of states (DOS) calculated for zigzag (left panel) and armchair (right panel) DWZnSNTs of different sizes : (a) (8,0)(8,0), (b) (10,0)(10,0), (c) (12,0)(12,0), (d) (14,0)(14,0), (e) (16,0)(16,0), zigzag nanotubes and (f) (4,4)(4,4), (g) (5,5)(5,5), (h) (6,6)(6,6), (i) (7,7)(7,7), (j) (8,8)(8,8) armchair nanotubes.

of individual atoms in the DOSs shows that inner wall atoms have contribution to each of valence band but contribute only to the bottom of the conduction band.

In Figure 10 we have shown the variation of band gap of DWZnSNT as a function of mean radius of the tube. The band gaps of both zigzag and armchair nanotubes show an overall increasing trend with the radius of the tube. The armchair nanotubes

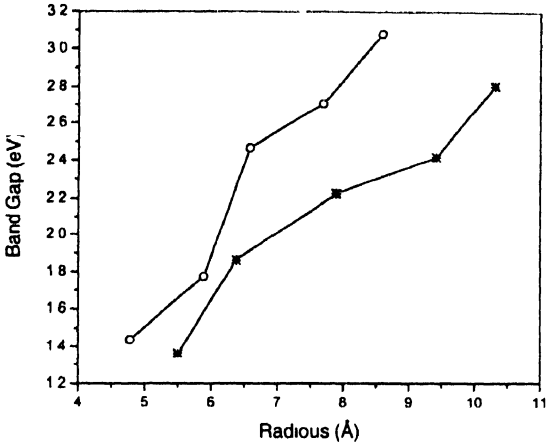

Figure 10. Band gaps of double-walled (a) armchair and (b) zigzag nanotubes as a function of the tube mean radius Circles (0) for armchair and crosses (x) for zigzag nanotubes.

have higher band gap values than that of zigzag tubes of comparable size. The increase in band gap with increasing tube radius may be related to the curvature induced $\sigma - \pi$ hybridization in the nanotubes with different radius. Another important result is that DWZnSNTs have lower band gap values compared to SWZnSNTs. The reduction of the gap is mainly due to the band shift of the inner and outer tubes, which is in turn due to the difference in $\sigma - \pi$ hybridisation for the tubes. The energy bands of the inner tube are shifted below relative to those of outer tubes. The interwall interactions break the degeneracy of the valence band maximum states which also contributes to the reduction of the energy gap. This reduction of energy gap is more significant for armchair nanotubes. However, the reason behind this is yet unclear to us. More detailed studies need to be done to understand the effect of the curvature and interwall interactions in DWNT.

4. Conclusions

In conclusion, we have studied the structural, electronic and optical properties of both single walled and double walled ZnS nanotubes with zigzag and armchair symmetry as a function of tube radius. The study of radial distribution suggests the presence of certain degrees of buckling in the nanotubes and it decreases with increasing tube radius for SWZnSNT while increases for DWZnSNT. We have found uniform charge transfer from Zn to S in SWZnSNT while for double-walled nanotube the charge transfer for inner wall atoms are less than that of outer wall atoms. In DWZnSNT, the charge transfer occurs from inner wall to outer wall. For SWZnSNT, the band gap decreases with increasing tube radius for zigzag ZnS nanotube while it increases for armchair nanotubes. The band gap of DWZnSNTs are lower than that of SWZnSNTs and the presence of interwall interaction is primarily responsible for the reduction of the band gap values. Because of curvature induced $\sigma - \pi$ hybridisation, the band gap of

DWZnSNTs increases with increasing tube radius for both zigzag and armchair symmetry. In total, our study reveals a fascinating and rich nanochemistry of tubular forms of ZnS semiconductor, which we hope would merit detailed experimental investigation.

Acknowledgments

The financial support from CSIR, Government of India [01(2148)-EMR-II/2007], UGC, New Delhi (though SAP scheme), DST, Government of India through FIST are gratefully acknowledged. One of the authors (S P) is grateful to CSIR, for the award of Senior Research Fellowship (SRF).

References

[1] H S Nalwa (Ed.) *Handbook of Nanostructures Materials and Nanotechnology* (San Diego, CA : Academic Press) (2000)

[2] J Hu, T W Odom and C M Lieber *Acc. Chem. Res.* **32** 435 (1999)

[3] P D Yang and C M Lieber *Science* **273** 1896 (1996)

[4] S Iijima *Nature* (London) **354** 56 (1991)

[5] M Ouyang, J L Huang, C L Cheung and C M Lieber *Science* **292** 702 (2001)

[6] P G Collins, M S Arnold and P Avouris *Science* **292** 706 (2001)

[7] J W Mintmire, B I Dunlap and C T White *Phys. Rev. Lett.* **68** 631 (1992)

[8] N Hamada, I S Sawada and A Oshiyama *Phys. Rev. Lett.* **68** 1579 (1992)

[9] M Remskar *Adv. Mater.* **16** 1497 (2004)

[10] R Tenne, L Margulis, M Genut and G Hodges *Nature* **360** 444 (1992)

[11] A Rubio, J L Corkill and M L Cohen *Phys. Rev.* **B49** 508 (1994)

[12] M Cote, M L Cohen and D J Chadi *Phys. Rev.* **B58** R4277 (1998)

[13] D Zhang and R Q Zhang *Chem. Phys. Lett.* **371** 426 (2003)

[14] S M Lee, Y H Lee, Y G Hwang, J Elsner, D Porezag and Th. Fraunheim *Phys. Rev.* **B60** 7788 (1999)

[15] C Ghosh, S Pal, B Goswami and P Sarkar *J. Phys. Chem.* **C111** 12284 (2007)

[16] M Zhao, X Yueyuan, L Feng, R Q Zhang and S -T Lee *Phys. Rev.* **B71** 085312 (2005)

[17] O Ponomarchko, M W Radny, P V Smith and G Seifert *Phys. Rev.* **B67** 125401 (2003)

[18] G Seifert, H Terrones, M Terrones, G Jungnickel and Th Frauenheim *Phys. Rev. Lett.* **85** 146 (2000)

[19] E Hernandez, C Goze, P Bernier and A Rubio *Phys. Rev. Lett.* **80** 4502 (1998)

[20] M W Zhao, Y Y Xia, D J Zhang and L M Mei *Phys. Rev.* **B68** 235415 (2003)

[21] L V Zavyalova, A K Savin and G S Svechnikov *Displays* **18** 73 (1997)

[22] T A Bendikov, C Yarnitzky and S Licht *J. Phys. Chem.* **B106** 2989 (2002)

[23] W Z Tang and C P Huang *Water Res.* **29** 745 (1995)

[24] X D Wang, P X Gao, J Li, J S Xhristopher and Z L Wang *Adv. Mater.* **14** 1732 (2002)

[25] Y C Zhu, Y Bando and Y Uemura *Chem. Commun.* 836 (2003)

[26] Y Jiang, M Xiang-Min, J Liu, Z-R Hong, C-S Lee and S-T Lee *Chem. Mater.* **15** 1195 (2003)

[27] H Zhang, S Zhang, S Pan, G Li and J Hou *Nanotechnology* **15** 945 (2004)

[28] S Pal, B Goswami and P Sarkar *J. Phys. Chem.* **C111** 1557 (2007)

[29] D Porezag, Th Frauenheim, Th Kohler, G Seifert and R Kaschner *Phys. Rev.* **B51** 12947 (1995)

[30] S Pal, B Goswami and P Sarkar *J. Chem. Phys.* **123** 044311 (2005)

[31] X Blase, L X Benedict, E L Shirley and S G Louie *Phys. Rev. Lett.* **72** 1878 (1994)

[32] S Reich, C Thomsen and P Ordejon *Phys. Rev.* **B65** 155411 (2002)

[33] H Liu, G Zhou. Q Yan, J Wu, B-L Gu, W Duan and D-L Zhao *Phys. Rev.* **B75** 125410 (2007)